Journal of Applied Polymer Science

Separation of Acetic Acid from Dilute Aqueous Solution by Nanofiltration Membrane

Kundan Baruah, Swapnali Hazarika
Chemical Engineering Division, CSIR-North East Institute of Science and Technology, Jorhat 785 006, Assam, India
Correspondence to: S. Hazarika (E-mail: shrrljt@yahoo.com)

ABSTRACT: NF membranes have been prepared from α, β, γ-cyclodextrin (CD) composite with polysulfone and characterized by pore size, thickness, pure water permeability, contact angle measurement and membrane morphology study. The permeation performances of the prepared membranes have been tested for separation of acetic acid from dilute aqueous solution. Effect of concentration, pressure, flow rate on flux and rejection have been calculated and interpreted. Different permeation models have been tested for experimental values and validated by comparing the values with the experimental data. It has observed that in β-CD membranes 99% recovery of acetic acid from aqueous solution has been obtained and found to be the best membrane for separation of acetic acid from dilute solution. © 2014 Wiley Periodicals, Inc. J. Appl. Polym. Sci. **2014**, *131*, 40537.

KEYWORDS: composites; films; membranes; separation techniques

Received 1 August 2013; accepted 31 January 2014
DOI: 10.1002/app.40537

INTRODUCTION

Owing to their distinctive features such as low costs, low energy, and as a solution to long standing problems in chemical industries, membrane technologies have been widely applied in chemical and biochemical process stream separation, purification, recovery, seawater desalination, removal of heavy metals from waste effluents, purification of potable water[1,2] etc. Nanofiltration (NF), which emerged in the mid-1980s, is a pressure-driven process that represents the transition between ultrafiltration (UF) and reverse osmosis (RO). It has the advantage of low operating pressure compared to RO and higher molecular weight retentions compared to UF. For this reason, NF has been widely applied in many industrial fields such as solvent recovery from lube oil[3] and vegetable oil[4] filtrates in pharmaceutical industry and for solvent exchange in the chemical industry.[5]

In Fine chemical industry, organic solvents are liberated with the industrial effluent. Most notably in the process stream of polyester industry and ethanol industry, low concentrated acetic acid is liberated with the process stream. Several methods are available to remove acetic acid from the process stream. Examples of such processes include distillation, extraction, neutralization, over-liming, vacuum evaporation, stream stripping, charcoal adsorption, ion exchange resin adsorption etc.[6,7] Recently, membrane processes such as adsorptive membrane and membrane extraction have been used to remove acetic acid from the process stream. Processes like distillation, solvent extraction, adsorption etc. are high energy extensive process.[5–7] As the distribution coefficient and solubility of acetic acid between the two phases (i.e., organic and aqueous system) is low, the amount of solvent required for extraction is very high and economically ineffective. Moreover, distribution coefficient will change due to ionization of acetic acid. Application of membrane technology for removal of acetic acid is an efficient process but still in its infancy. To the best of our knowledge, there are a few investigations on NF separation of acetic acid on downstream processing.[8] However, transport and retention data for NF membranes in organic solvents are very limited in the literature and the mechanism of transport through NF membranes in organic solvent environment is not well understood. Previous studies have shown that nanofiltration (NF) is one of the effective technologies to remove organic compounds when the solute size are larger than the membrane pore size or organic compounds have ionizable functional groups causing electrostatic repulsion.[9–11] However, these studies have typically considered relatively large compounds (e.g., M.W. $>$ 150 g mol^{-1}) and/or relatively hydrophobic compounds (e.g., Logarithm of octanol-water partition coefficient $>$ 2.0). Only a few studies have investigated the rejection of small uncharged organic compounds by NF membranes.[12–14] A complete understanding of the transport of small organic compounds through NF membranes is a challenging issue, since solute transport depends on physico-chemical properties of the solvent, solute and membrane. Several recent studies have investigated the transport mechanism of organic solutes through NF membranes. These studies have shown that for organic compounds

the removal depends upon the solute size and shape, polarity or hydrophobicity, the membrane pore size, and charge. Thus, to save energy and improve the quality of product NF technique was introduced for recovery of acetic acid which is a new process in membrane separation and its application have been increasing rapidly in the last decade.

In this article, we report a comprehensive study on NF membrane through removal of acetic acid from dilute aqueous solution of acetic acid (≤3%). NF membranes were prepared indigenously from α, β, and γ-cyclodextrin composite with polysulfone and characterized. Selection of Cyclodextrin is based on unique characteristics of uniform macromolecular structure, molecular self assembling etc.[15] Because of its ability to form host guest complexes with organic components having appropriate diameters and physical interactions, it can also be used for studying host guest chemistry.[16,17]

In the literature, different solvent, solute and membrane parameters influencing the transport model were experimentally identified and different models were developed.[12–14,18–24] However, transport models for Nanofiltration system are limited for specific experimental data. Therefore further research and improvement of transport models are highly necessary. For our work, permeation results were analyzed through a suitable permeation model and the effects of solvent membrane parameters were identified.

MATERIALS AND METHODS

Polysulfone (average molecular weight 22,000, purity 99%) was obtained from Aldrich Chemical Company, USA in pellet form. Polyethylene glycol 1500 was supplied by G.S. Chemical testing Lab & Allied Industries, India. α, β, and γ-cyclodextrin hydrate (purity 99%) and lithium nitrate (99% extra pure) were supplied by Acros Organics, USA. *N*-methyl pyrrolidone (NMP, purity > 99.5%) was procured from Rankem, India. All reagents were used without any further purification.

Membrane Preparation

Flat sheet membranes were prepared by dissolving Polysulfone (PSf) in NMP as solvent at room temperature (28–32°C and relative humidity about 78%) and then mixed with definite amount of Polyethylene glycol (PEG-1500) used as additive, $LiNO_3$ as swelling gel, and α, β, γ-cyclodextrin separately to make the casting solution. Compositions and physical properties of the casting solution for preparation of membrane are given in Table I. The polymer solution was stirred for about 6 h at room temperature (28–30°C) using a magnetic stirrer until a homogeneous solution was achieved. Films were cast on a glass plate with a casting Knife maintaining the same temperature as in the solution and are exposed for about 5 min to ambient before immersion into a coagulation bath that contains ice-cooled water (maintained at about 6°C). Then the membranes were immersed into the coagulation bath and kept out from the glass plate after sometime. The prepared membrane sheets were washed under running water and kept in deionized water bath overnight. Then the sheets were dried at room temperature. Finally the membranes were characterized by using different analytical methods and kept ready for permeation experiments.

Measurement of Membrane Separation Performance

Rejection and fluxes were determined using a disproportionate two-compartment membrane cell whose compartment volume on the feed side and permeate side was 200 and 100 mL, respectively. The polymeric membrane was placed between the compartments with silicone-rubber packing and the cell was connected with a reservoir of 500 mL. The effective membrane area is 15 cm^2. Aqueous solutions of acetic acid was stirred continuously and circulated by peristaltic pump. Three experiments were conducted for each selection of the optimum conditions (pressure, temperature, flow rate and concentration). All permeation experiments were carried out in a batch mode for 2 h. The sample solutions were collected from the permeate side after a permeation period and analyzed by titration method. The separation performance of NF membranes depends on the operating conditions such as pressure, temperature, flow rate, and concentration.[25] A self made batch experimental set up was used to study the separation performance of NF membrane and the schematic diagram is shown in Figure 1.

Analytical Methods

The membranes were characterized for pore size, porosity, thickness, and surface morphology by using same methods reported in our previous publication.[26] Pore diameter and porosity of the membranes were determined by Capillary Condensation flow porometer (PMI, Model CCFP-5A). The principle of this process is that at a pressure P_o, of vapor in equilibrium with its liquid can condense in pores of material. Vapor condenses in all pores smaller than D (pore diameter), determined by the pressure of the vapour.[26]

$$D = -[4\gamma v \cos\theta / RT)]/\ln(P/P_\circ) \quad (1)$$

where γ is the surface tension of condensed liquid, v is the molar volume of condensed liquid, θ is the contact angle of the liquid with the pore, D is the pore diameter, R is the gas constant, and T is the absolute test temperature. At the lowest relative vapor pressure, (P/P_o), condensation occurs in the smallest pore. On increase of relative vapor pressure condensation occurs

Table I. Composition and Physical Properties of the Composite NF Membranes

% of membrane material		% of polysulfone	% of $LiNO_3$	% of PEG	% of NMP	Membrane thickness (μm)	Pore diameter (nm)	Surface porosity (ε%)	Pure water permeability (L m^{-2} h^{-1})	Water uptake (%)	Contact angle (°)
Alpha-CD	0.402	16.166	0.161	0.483	82.836	57.40	32.6	0.14	48×10^{-5}	8.36	38
Beta-CD	0.378	11.344	0.196	1.134	86.946	12.30	38.4	0.37	43×10^{-5}	6.29	45
Gama-CD	1.022	15.337	0.306	1.533	84.355	64.80	59.1	0.52	39×10^{-5}	4.98	57

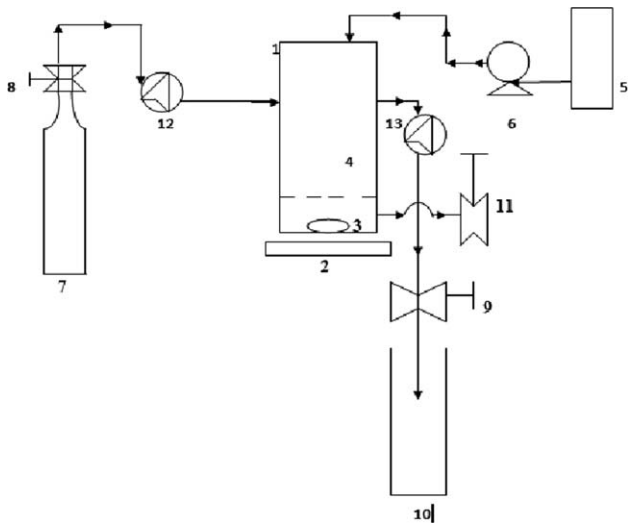

Figure 1. Flow diagram of permeation experiment. Membrane cell 2. Magnetic stirrer 3. Magnetic capsule 4. Membrane 5. Feed tank. Peristaltic pump 7. N_2 gas 8. Gas valve 9. Gas valve 10. Water vessel 11. Sample collecting valve 12. Pressure gauze 13. Pressure gauze.

in larger pores. A small increase in pressure on inlet side of the sample causes flow. Measurement of pressure change in outlet side of the sample yields flow rate.

$$F_{\mathrm{STP}} = (\gamma Ts/TPs)(\mathrm{d}p/\mathrm{d}t) \tag{2}$$

After obtaining the value of vapor equilibrated with the sample and rates of pressure change, the pore diameter of the nanopore membrane were obtained.

The thicknesses of the prepared membranes were measured by a membrane thickness gauge made by Mitutoyo Corporation Japan. Membrane morphology was studied by a scanning electron microscope (SEM) (LEO 1400VP, UK) and Transmission Electron Microscope (TEM) (JEOL, Japan, JEM 2100) at an accelerating voltage of 200 kV, which directly provides the visual information of the membrane morphology such as pore shape, size, their distribution and density. Pure water permeability for all membranes was measured in a membrane cell of standard design.[26] The membranes with effective area of 15 cm^2 were set in the test cell and the pure water permeability test was carried out by applying compressed high-purity nitrogen gas to the feed side. The quantity of water permeated through the membrane was measured as permeation rate (L m^{-2} h^{-1}). Contact angles of the membranes were measured by bubble formation method applying Poiseuille's equation which expresses the balance between viscous forces and capillary and hydrostatic forces (neglecting inertial effects) and reported in our previous communication.[26] Qualitative information regarding surface and cross sectional morphology of the prepared membranes was obtained through SEM and TEM analysis.

THEORETICAL BACKGROUND

Permeation Flux and Rejection

The separation performance of NF membranes depends on the operating conditions such as pressure, temperature, flow rate and concentration. For a batch experimental set up the permeation flux was calculated by the following equation,[27]

$$J = \frac{V}{A\Delta t} \tag{3}$$

The percent rejection can be defined by,[28]

$$R_{\mathrm{obs}}\,\% = 1 - \frac{C_p}{C_F} \tag{4}$$

Permeation Model

In the nanofiltration systems, some studies support the use of pore flow model and some others support the solution diffusion model. The simplified version of both the models was given by Silva et al.[29]

Pore-Flow Model. As reported by Silva et al.,[29] it is assumed that the stable pores to be present inside the membrane and the driving force across the membrane is the pressure. At constant temperature, we can write,

$$-\chi_{i(m)}\nabla_{T,P}\mu_i - \chi_{i(m)}\bar{V}_i\nabla p = \sum_k \zeta_{i,k}\frac{\chi_{k(m)}N_i}{c_{i(m)}(\varepsilon/\tau)} + \zeta_{i,m}\frac{N_i}{c_{t(m)}(\varepsilon/\tau)} + \alpha_i'\frac{\zeta_{i,m}x_{i(m)}\beta_\circ}{\eta}\nabla p \tag{5}$$

If the pressure gradient contribution is more significant than the activity gradient to the transport then eq. (5) is simplified to

$$-\chi_{i(m)}\bar{V}_i\nabla p - \alpha_i'\frac{\zeta_{i,m}x_{i(m)}\beta_\circ}{\eta}\nabla p = \sum_k \zeta_{i,k}\frac{\chi_{k(m)}N_i}{c_{i(m)}(\varepsilon/\tau)} + \zeta_{i,m}\frac{N_i}{c_{t(m)}(\varepsilon/\tau)} \tag{6}$$

When friction of acetic acid with the membrane is much higher than the friction between acetic acid and water then we can write,

$$-\chi_{i(m)}\bar{V}_i\nabla p + \alpha_i'\frac{\zeta_{i,m}x_{i(m)}\beta_\circ}{\eta}\nabla p = -\zeta_{i,m}\frac{N_i}{c_{t(m)}(\varepsilon/\tau)} \tag{7}$$

As the first term in the left side of eq. (7) is much lower than the second, thus the equation can be written as,

$$N_i = -\alpha_i'\frac{c_{i(m)}\beta_\circ}{\eta}\frac{\varepsilon}{\tau}\nabla p \tag{8}$$

For small permeating species in relation to the pore size, the total volume flux is given by

$$N_v = \frac{\beta_\circ}{\eta}\frac{\varepsilon}{\tau}\nabla p \tag{9}$$

where β_o is the specific permeability which is depend on membrane structure. When membrane is composed of more or less cylindrical pores then, Hagen–Poiseuille equation will be obtained,

$$N_v = -\frac{d_{\mathrm{pore}}^2}{32\eta}\frac{\varepsilon}{\tau l}\nabla p \tag{10}$$

If membrane consists of packed bed of particles, then Carman Kozeny equation will be obtained.

$$N_v = -\frac{d^2_{\text{particle}}}{180(1-\varepsilon)^2\eta}\frac{\varepsilon^3}{\tau l}\nabla \text{p} \tag{11}$$

Solution Diffusion Model. Considering concentration gradient,[29] it is assumed that each permeating molecule dissolves in the membrane phase and diffuses through the membrane. For this type of system, eq. (5) can be written as,

$$-\chi_{i(m)}\nabla_{T,P}\mu_i = \sum_k \zeta_{i,k}\frac{x_{k(m)}N_i - x_{i(m)}N_k}{c_{t(m)}} + \zeta_{i,m}\frac{x_m N_i}{c_{t(m)}} \tag{12}$$

Assuming that friction of species with the membrane is greater than the magnitude of the friction between species, then eq. (12) becomes,

$$-\chi_{i(m)}\nabla_{T,P}\mu_i = \zeta_{i,m}\frac{x_m N_i}{c_{t(m)}} \tag{13}$$

Neglecting kinetic coupling and approximating the gradient of chemical potential, eq. (13) simplifies to

$$N_i = -\frac{c_{i(m)}}{x_m\zeta_{i,m}}\nabla x_{i(m)} \tag{14}$$

Integrating eq. (14) and applying proper boundary conditions as applied by Silva et al.,[29] we obtain

$$N_i = P^{\text{molar}}_{i,m}\left(x_{i,f} - \frac{\gamma_{i,p}}{\gamma_{i,f}}x_{i,p}\exp\left(-\frac{\bar{V}_1\Delta p}{RT}\right)\right) \tag{15}$$

RESULTS AND DISCUSSION

Characterization of Membrane

CD-membranes were characterized for pore size, porosity, surface morphology, and pure water permeability. Some physical properties such as membrane thickness, pore diameter, surface porosity and pure water permeability of membranes are shown in Table I. Figure 2 shows the SEM image of the cross section of α-CD, β-CD, and γ-CD membranes. It is seen from the figure that α-CD, β-CD, and γ-CD membranes have asymmetric structure consisting of a dense top layer and a porous sub layer. The sub layer seems to have finger-like cavities as well as macrovoid structure. This finger like cavity is due to instantaneous demixing of membrane material in the solvent.[30] The SEM image of β-CD membrane shows a more regular image of surface morphology. A more continuous morphology is observed in the surface of this membrane than α-CD, and γ-CD membranes. The variation of membrane morphology for α-CD, β-CD, and γ-CD membranes is probably due to the difference in interaction between α-CD, β-CD, and γ-CD with the casting solvent. SEM image of top surface of the membranes are presented in Figure 3. The formation of the membrane top surface is probably a result of spinodal demixing because the diffusion processes during formation of the top layer are fast enough for the

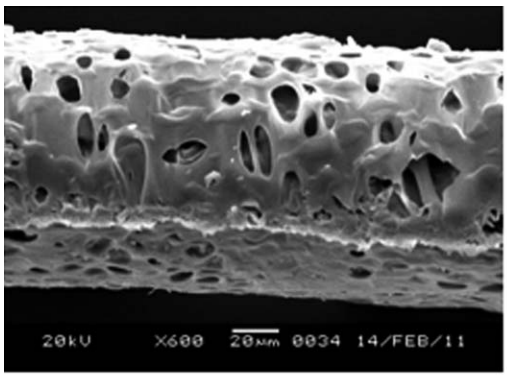

Alpha CD

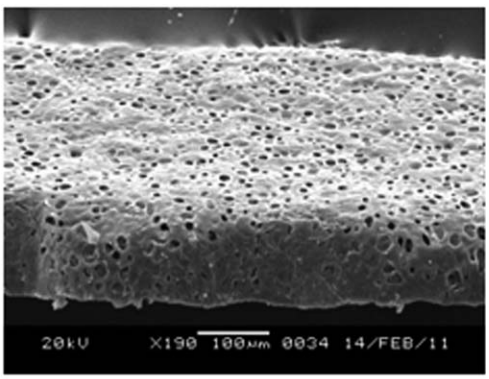

Beta CD

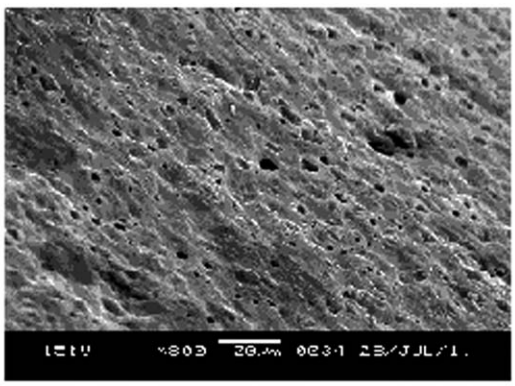

Gama CD

Figure 2. SEM photograph of side view of NF membrane. Alpha CD, Beta CD, Gama CD.

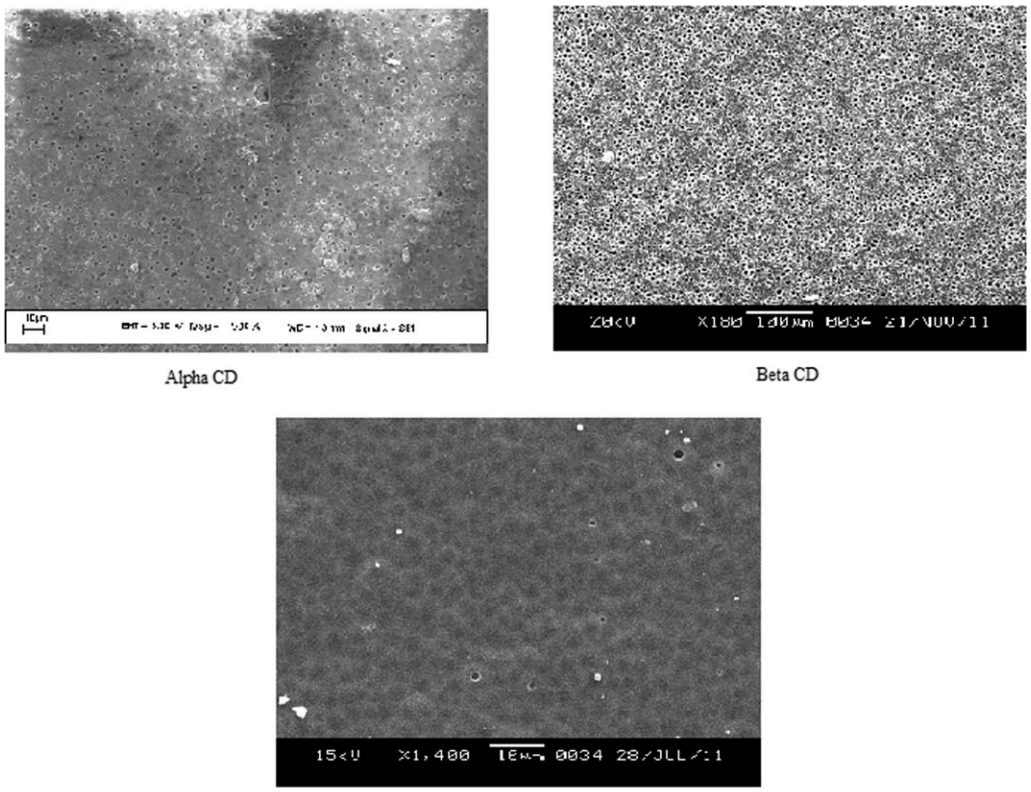

Figure 3. SEM photograph of front view of NF membrane. Alpha CD, Beta CD, Gama CD.

polymer solution to become a highly unstable and cross the spinodal curve decomposition.[31] This results a top surface with much better interconnected pores, which is more prominent in β-CD membrane. Thus, much better interconnectivity of pores in the membranes is achieved due to spinodal decomposition.

In Figure 4, TEM pictures of CD membranes are shown. To investigate the similarities and differences among the three membranes qualitatively, image analysis is performed on representative TEM pictures of α-CD, β-CD, and γ-CD membranes. From the TEM pictures it is seen that β-CD membranes contain more interstitial cavities than α-CD and γ-CD membranes. The interstitial cavities are interconnected in β-CD membranes, forming channels throughout the entire thickness of the membrane. This difference significantly reflected the difference in permeability of the membranes. Thus, creating interstitial mesopores in polymer nanocomposites is important to prepare highly permeable membranes while the aggregate structure has to be carefully designed.[32,33]

Effect of Concentration of Acetic Acid

To study the effect of concentration of acetic acid on permeation process, experiments were carried out in the concentration range from 0.174 mol L^{-1} (1 wt %) to 1.223 mol L^{-1} (7 wt %). From Figure 5, it is seen that the permeation flux declined slowly before the concentration reached at 0.611 mol L^{-1} (3.5%). This result shows that concentration of feed solution has a great influence on the separation performance of NF membranes. The permeation flux falls slowly with rising concentration when the concentration is over 0.611 mol L^{-1} (3.5%). The steady permeation flux reached at 83.9 L m^{-2} h^{-1} for β-CD membrane at high concentration, indicates that CD-polysulfone composite NF membrane has the potential in commercial applications for recovery of acetic acid from dilute aqueous solution. Similarly, the rejection is high (over 99%) and is scarcely affected by the concentration of acetic acid as shown in the same figure.

Effect of Pressure

Operating pressure is an important factor which influences separation performance. Generally, high operating pressure results in high permeation flux.[34] The relationship between operating pressure and separation performance for CD-polysulfone composite NF membrane is shown in Figure 6. The permeation flux at 1 bar is 84.5 L m^2 h^{-1} and it increases quickly with rising pressure and reaches 89.2 L m^2 h^{-1} at 5 bar. The phenomenon of flux increasing with pressure has been observed in other reports also: *n*-hexane flux increased with pressure as reported by Bhanushali,[24] flux of *n*-heptane and xylene (mixture of isomers) with pressure as reported by Robinson et al.,[35] flux of benzene and toluene went up with pressure was reported in White's study.[36] This illustrates that pressure boost is an effective method for increasing permeation flux. But it is seen from Figure 6 that permeation flux is not in proportion to the operating pressure. In other words, the increasing rate of the permeation flux diminishes during a rise in pressure. This may result from compressing effect of the membrane, and observed in other membrane separation processes also.[37,38] The average pore

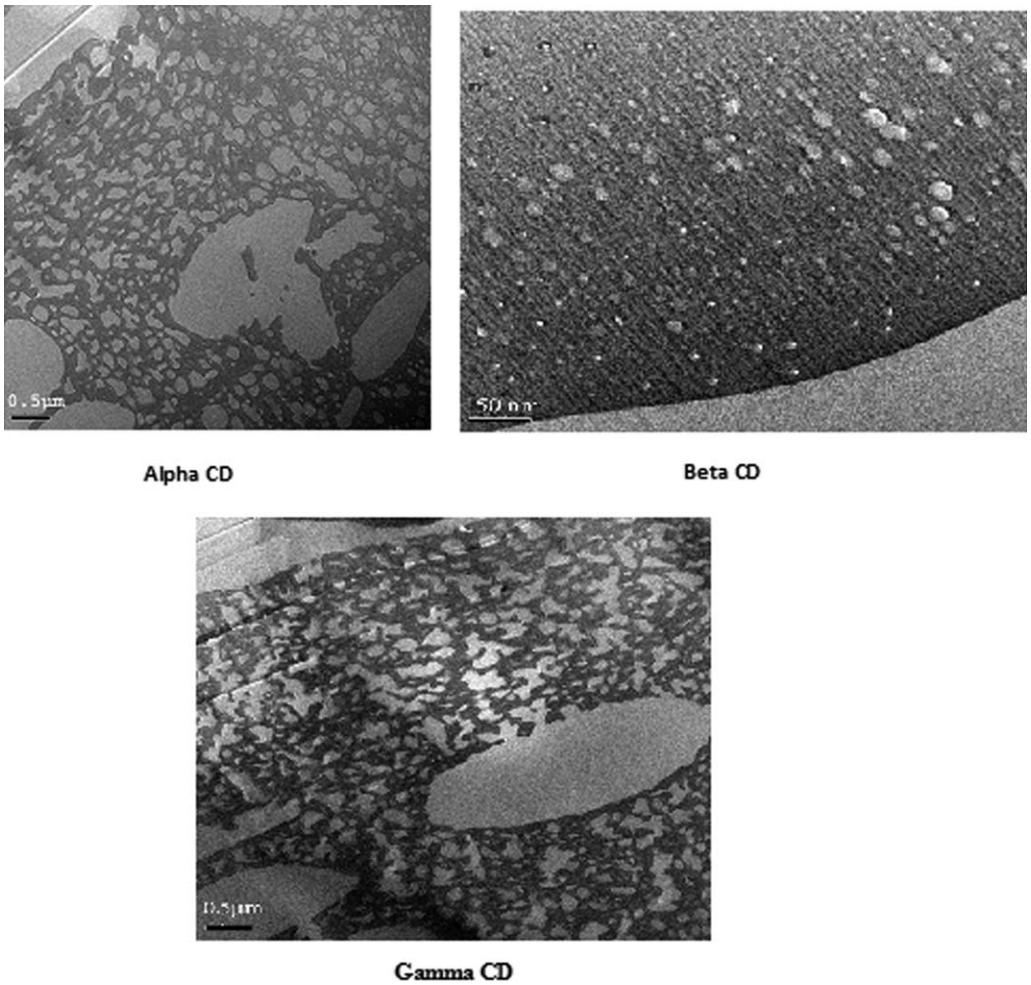

Figure 4. TEM photograph of NF Membrane. Alpha CD, Beta CD, Gama CD.

size of the active separation layer of membrane diminishes at high pressure. This may delay the increase in the transport rate for components with an increase in pressure and can increase the rejection. Therefore, very high pressure is not necessary to get a high transport rate. Higher pressure needs a higher investment of equipment and results in higher operational costs. A suitable operating pressure for this membrane separation system is found to be 3.5 bar. Permeation flux at 3.5 bar is observed to be 88.8 L m^2 h^{-1} and slightly less than the permeation flux at 5 bar, which is large enough for commercial

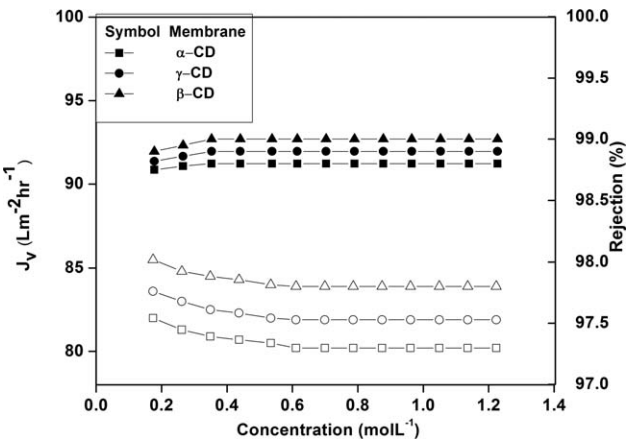

Figure 5. Flux and Rejection as a function of concentration of acetic acid. Open symbol: Flux, Closed symbol: Rejection.

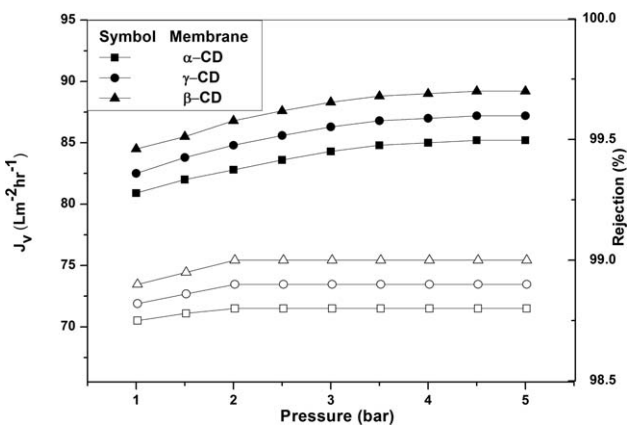

Figure 6. Flux and rejection as a function of operating pressure. Open symbol: rejection, closed symbol.

application. The rejection of acetic acid was as high as 99% as evident from Figure 6. The pressure is found to be little influence on the rejection for the separation process as the rejection is over 99%, even if at low pressure range.

Effect of Flow Rate

Flux of the membrane depends on flow rate of the solution. The fluid velocity near to the membrane surface is very small. A boundary layer exists at the interface of membrane and fluid. Flow in this part of the boundary layer is laminar and the mass transfer coefficient of each component in boundary is small. Thus, the thickness of the boundary layer influences the transport rate of the components from the bulk of feedstock to the surface of the membrane and further affects the permeation rate through the membrane. The thickness of the boundary layer of the membrane is related to the viscosity and the flow pattern of the fluid. With increasing the viscosity of the solution, the thickness of the boundary layer increases, as viscosity is a function of temperature and the operating temperature is restricted by the process conditions and is fixed at a stable value. The flow rate of the solution is a variable in the operation process, a high flow rate brought an ideal turbulent flow with a favorable flow pattern to reduce the thickness of the boundary layer. A high flow rate increases the tangential and radial velocity of fluids. The strong disturbance of fluid can break down the boundary layer at a certain extent. Therefore, increasing the flow rate is an effective factor to raise permeation flux, especially for those solutions where viscosities are not very low.

The effect of flow rate of aqueous acetic acid solution on the separation performance of membrane is shown in Figure 7 wherein the rejection is also shown for three types of NF membrane. The change in flow has not influenced the rejection; however it has little impact on permeation flux. The permeation flux increases when the feedstock flow rate goes up, which indicates that the mass transfer resistance exists in the boundary layer, and a high flow rate can reduce the resistance; but the range of permeation flux from 84.5 to 87 L m^2 h^{-1} is narrow, which means the boundary layer conditions is not very thick. The viscosity of the solution at a low concentration i.e., 2% is too low to form a thick boundary layer. Thus, the change of the flow rate has no significant impact on the variation of the thin boundary layer.

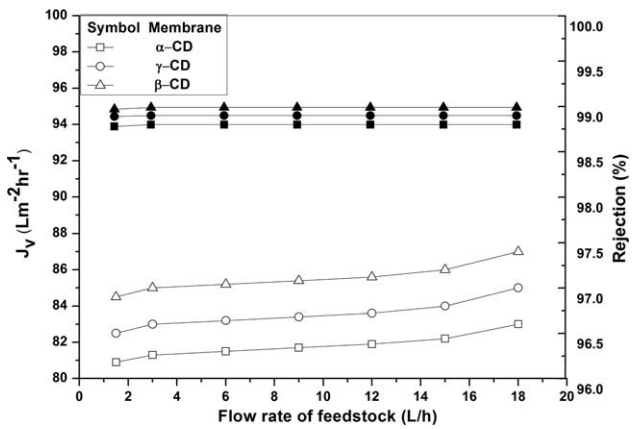

Figure 7. Flux and rejection as a function of flow rate. Open symbol: flux, closed symbol: rejection.

Effects of Operation Time

The expected useful lifetime of membranes is one of the critical questions which determine whether the membrane can be used commercially. Some kinds of polymer membranes have excellent separation performance, but they do not have a good solvent-resistant property, which can be typically found in the significantly decreased rejection after a long period of operation. Experiments were carried out to demonstrate membrane stability in acetic acid and tested long-term performance of the membranes over a period of 4 months. From Figure 8 it is seen that, the separation performance was kept at a high level after a long period of work. Permeation flux decreased from 84.5 L m^2 h^{-1} to a steady state of 83.5 L m^2 h^{-1}. The slight decline of flux is due to membrane compaction at 3 months. The densification of the membrane under pressure reduced the flux through the membrane. Long-term operation has little influence on the rejection of acetic acid as shown in the same figure, which indicates that the solvent-resistant performance of β-CD NF membrane is good.

Effect of Concentration Polarization

In membrane filtration processes, some of the components in the solution are rejected by the membrane and accumulate near the membrane surface. Before reaching a steady state the convective flow of the components to the membrane surface is larger than that due to diffusion back-flow to the bulk solution. This phenomenon is called concentration polarization. The effect of concentration polarization can give the concentration of solution at the surface of the membrane. We have omitted the effect of friction of acetic acid with the porous membrane matrix, at constant temperature and the solution viscosity. In this case, the ratio of the net transmembrane pressure across the membrane is equal to the ratio of the product rate (P_r) to the pure water permeability (P_w). For pure water permeation, the net transmembrane pressure is considered to be the applied pressure (∇p). This concept can be applied for the Poisseuille flow within the membrane pores or Darcy's law

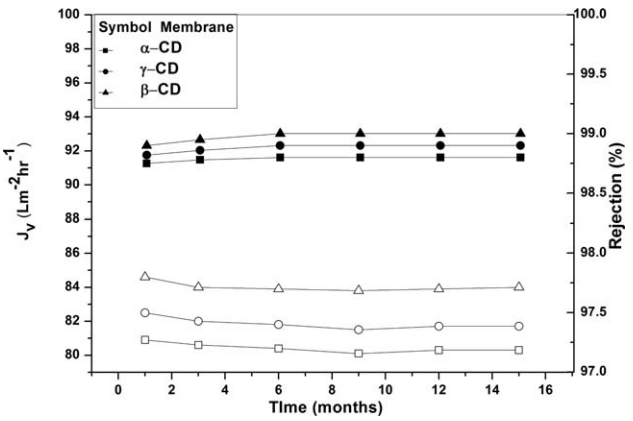

Figure 8. Effect of operation time on permeation flux and rejection (3.5 bar, temp:25°C, feedstock flowrate: 100 mL min^{-1}, concentration of acetic acid: 0.349 mol L^{-1}). Open symbol: flux, closed symbol: rejection.

for describing solute transport through the porous membrane matrix.[39]

The actual trans membrane pressure is given by,

$$\left[\nabla p - \prod C_o + \prod C_l\right], \tag{16}$$

where ΠC_o and ΠC_l are the osmotic pressures at the entrance and exit of the membrane pores.

Now,

$$\frac{P_r}{P_w} = \frac{(\nabla p - (\prod C_o + \prod C_l))}{\nabla p} \tag{17}$$

Thus, the boundary layer concentration C_o which accounts for the reduction in product rate is 45 mol L^{-1}, whereas the initial feed concentration is only 1.223 mol L^{-1}. Since the surface concentration which is three orders of magnitude larger than bulk quantities are unreasonable and hence concentration polarization cannot explain in this case.

Transport Model Fitting and Statistical Analysis

Two described models mentioned in Permeation Model section have been used to analyze the flux data given in Figure 5. In the Pore Flow model the permeability term $\frac{d_{\text{pore}}^2}{32\eta}\frac{\varepsilon}{\tau l}$, given in eq. (10) has been determined by the physical properties of the membrane and this value is 4.2 $\times$ 10^{-15} m for acetic acid. The predicted values using both pore flow and solution diffusion models are shown in Figure 9. It is clear that pore flow model provides much better predictions for acetic acid system. However, in case of binary mixtures of the solvent solution diffusion model better predicts the solvent fluxes.[29] Better predictions of solution diffusion model than pore flow model in binary solvent system is due to the degree of separation. In pore flow model, no solvent separation is expected while in solution diffusion model small solvent separation occurs through the permeate.[40] Thus, transport of acetic acid through β-CD NF membrane follows the pore flow model and can be used for the design of separation device for separating acetic acid from aqueous solution.

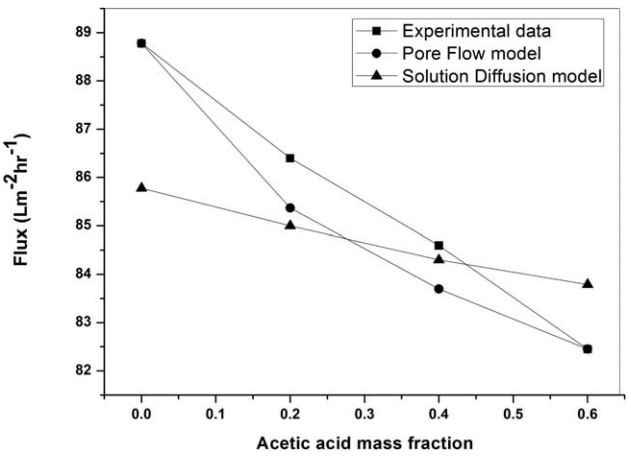

Figure 9. Comparison of experimental acetic acid flux data in β-CD membrane at pressure 2 bar (calculated values by solution diffusion and pore flow model).

SUMMARY

NF membranes are prepared from α, β, γ-cyclodextrin composite with polysulfone and characterized. The permeation performances of the prepared membranes were tested for recovery of acetic acid from dilute aqueous solution. Effect of concentration, pressure, flow rate on flux, and rejection are studied and optimum conditions were established. Suitable operating pressure for acetic acid recovery from dilute aqueous solution through polysulfone-composite β-CD membrane is 3.5 bar which is a suitable pressure range for commercial application. The rejection decreases when the feedstock flow rate goes up, which clearly indicates that the permeation flux increases due to the decrease in mass transfer resistance, as a result high flow rate was obtained. The activity of the membranes remains same up to 3 months. From the calculated and experimental values it was established that pore flow model is well fitted for separation of acetic acid from dilute aqueous solution.

LIST OF SYMBOLS:

J	permeation flux (L m^{-2} h^{-1})
R_{obs}	observed rejection
c	molar concentration (mol L^{-1})
d_{pore}	pore diameter (nm)
d_{particle}	particle diameter (m)
l	membrane thickness (nm)
N_i	molar flux (mol m^{-2} s^{-1})
N_v	total volume flux (m s^{-1})
J	solvent flux (L m^{-2} h^{-1})
∇p	applied pressure (bar)
Π	osmotic pressure (bar)
n	number of moles of acetic acid
V	volume of permeate in time t (mL)
$P^{\text{molar}}{}_{\text{im}}$	molar permeability (mol m^{-2} s^{-1})
R	ideal gas constant (Pa m^{-3} mol^{-1} K^{-1})
t	time (s)
T	temperature (K)
w	mass fraction
x	molar fraction
A	membrane area (cm^2)
ΔC	concentration variation in the corresponding aqueous solution at the time interval Δt
C_f	concentration of the feed (mol L^{-1})
C_p	concentration of the permeate side (mol L^{-1})
μ	chemical potential (J mol^{-1})
ρ	density (kg m^{-3})
τ	tortuosity factor
α'	viscous flow characterization parameter
β_o	membrane viscous flow characterization parameter
γ	molar activity co-efficient
δ	Hilderband solubility parameter ($MPa^{1/2}$)
ε	porosity
χ	Flory–Huggins interaction parameter
ζ	friction coefficient (J s^{-1} m^{-2} mol^{-1})
η	viscosity (Pa s^{-1})

ΠC_o osmotic pressure at the entrance of the membrane pores
ΠC_l osmotic pressure at the exit of the membrane pores

Subscripts

f feed side
i, *k* species
m, (*m*) membrane

ACKNOWLEDGMENTS

Financial support from DST-New Delhi, India, Grant No. SR/S5/GC-14/2008, dated May 22, 2009, has been gratefully acknowledged.

REFERENCES

1. TreVry-Goatley, K.; Buckley, C.; Groves, G. *Desalination* **1983**, *47*, 313.
2. Bhattacharyya, D.; Williams, M. E. Reverse osmosis: selected applications. In: Membrane Handbook; Ho, W. S. W.; Sirkar, K. K., Eds.; Van Nostrand Reinhold: New York, **1992**; p 265.
3. White, L. S.; Nitsch, A. R. *J. Membr. Sci.* **2000**, *179*, 267.
4. Cheryan, M. *Membr. Technol.* **2005**, *2*, 5.
5. Uekama, K. *Chem. Pharm. Bull.* **2004**, *52*, 900.
6. Jookim, K.; Urmila, M. D.; Tomazi, K. *Chem. Eng. Commun.* **2004**, *191*, 1.
7. Pandit, P.; Basu, S. *Ind. Eng. Chem. Res.* **2004**, *40*, 7861.
8. Ansthas, H. M.; Gaikar, V. G. *React. Funct. Polym.* **2001**, *47*, 23.
9. Kiso, Y.; Sugiura, Y.; Kitao, T.; Nishimura, K. *J. Membr. Sci.* **2001**, *192*, 1.
10. Nghiem, L. D.; Schafer, A. I.; Elimelech, M. *Environ. Sci. Ol.*, **2004**, *38*, 1888.
11. Nghiem, L. D.; Manis, A.; Soldenhoff, K.; Schafer, A. I. *J. Membr. Sci.* **2004**, *242*, 37.
12. Lee, S.; Lueptow, R. M. *Life Support Biosphys. Sci.* **2000**, *7*, 251.
13. Lee, S.; Lueptow, R. M. *J. Membr. Sci.* **2001**, *182*, 77.
14. Lee, S.; Lueptow, R. M. *Environ. Sci. Technol.* **2001**, *35*, 3008.
15. Crini, G.; Morcellet, M. *J. Sep. Sci.* **2002**, *25*, 789.
16. Groger, M.; Kretzer, E. K.; Woyke, A. Cyclodextrine; Science Forum Universitat: Siegen, **2001**; p 1.
17. Schmidt, R. Cyclodextrine; Justus-Liebig Universitat Gieen, **2003**; p 1.
18. Van der Bruggen, B.; Geens, J.; Vandecasteele, C. *Chem. Eng. Sci.* **2002**, *57*, 2511.
19. Lin, K. M.; Zhang, X. Y.; Koseoglu, S. S. *J. Food Lipids.* **2004**, *11*, 29.
20. Yang, X. J.; Livingston, A. G.; Freitas dos Santos, L. *J. Membr. Sci.* **2001**, *190*, 42.
21. Bhanushali, D.; Kloos, S.; Bhattacharyya, D. *J. Membr. Sci.* **2002**, *208*, 340.
22. Robinson, J. P.; Tarleton, E. S.; Millington, C. R.; Nijmeijer, A. *J. Membr. Sci.* **2004**, *230*, 29.
23. Geens, J.; Van der Bruggen, B.; Vandecasteele, C. *Chem. Eng. Sci.* **2004**, *59*, 1161.
24. Bhanushali, D.; Kloos, S.; Kurth, C.; Bhattacharyya, D. *J. Membr. Sci.* **2001**, *189*, 1.
25. Mulder, M. Basic Principles of Membrane Technology; Dordrecht: Kluwer Academic Publishers, **1996**; p 224.
26. Baruah, K.; Hazarika, S.; Borthakur, S.; Dutta, N. N. *J. Appl. Polym. Sci.* **2012**, *125*, 3888.
27. Zhaoan, C.; Maicun, D.; Yong, C.; Gaohong, H.; Ming, W.; Junde, W. *J. Membr. Sci.* **2004**, *235*, 73.
28. Han, S.; Wong, H. T.; Livingston, A. G. *Trans. IChem. E A Chem. Eng. Res. Des.* **2005**, *83*, 309.
29. Silva, P.; Shejiao, H.; Livingston, A. G. *J. Membr. Sci.* **2005**, *262*, 49.
30. Boom, R. M.; Wienk, I. M.; Boomgaard Van den, T.; Smolders, C. A. *J. Membr. Sci.* **1992**, *73*, 277.
31. Wienk, M.; Boom, R. M.; Beerlage, M. A. M.; Bulte, A. M. W.; Smolders, C. A. *J. Membr. Sci.* **1996**, *113*, 361.
32. Uragami, T.; Meotoiwa, T.; Miyata, T. *Macromolecules* **2003**, *36*, 2041.
33. Binyam, S.; Mukhtar, H.; La, K. K. *J. Appl. Polym. Sci.* **2010**, *10*, 3331.
34. Baker, R. W. Membrane Technology and Applications; Wiley: England, **2004**.
35. Robinson, J. P.; Tarleton, E. S.; Millington, C. R.; Nijmeijer, A. *J. Membr. Sci.*, **2004**, *230*, 29.
36. White, L. S. *J. Membr. Sci.* **2002**, *205*, 191.
37. Murthy, Z. V. P.; Gupta, S. K. *Desalination* **1997**, *109*, 39.
38. Murthy, Z. V. P.; Gupta, S. K. *J. Membr. Sci.* **1999**, *154*, 89.
39. Tam, C. M.; Tremblay, A. Y. *J. Membr. Sci.* **1991**, *57*, 271.
40. Silva, P.; Adam, W. J.; Luke, B.; Meares, P. *J. Membr. Sci.* **1983**, *13*, 127.